

End-to-End Differentiable Learning of a Single Functional for DFT and Linear-Response TDDFT

Xiaoyu Zhang¹

¹College of Chemistry and Molecular Engineering,
Peking University, Beijing 100871, the People's Republic of China*

(Dated: February 6, 2026)

Density functional theory (DFT) and linear-response time-dependent density functional theory (LR-TDDFT) rely on an exchange–correlation (xc) approximation that provides not only energy but also its functional derivatives that enter the self-consistent potential and the response kernel. Here we present an end-to-end differentiable workflow to optimize a single deep-learned energy functional using targets from both Kohn–Sham DFT and adiabatic LR-TDDFT within the Tamm–Dancoff approximation. Implemented in a JAX-based two-component quantum chemistry code (IQC), the learned functional yields a consistent potential and LR kernel via automatic differentiation, enabling gradient-based training through the SCF fixed point and the Casida equation. As a proof of concept in a fixed finite basis (cc-pVDZ), we learn an exchange-correlation functional on the helium spectrum while incorporating one-electron self-interaction cancelation and the Lieb–Oxford inequality as penalty terms, and we assess its possible transfer to molecular test cases.

Density functional theory (DFT) [1, 2] and its linear-response time-dependent extension (LR-TDDFT) [3, 4] provide an efficient route to ground-state and excitation energies for molecules and materials; yet, their predictive accuracy is ultimately limited by the exchange–correlation (xc) approximation. In Kohn–Sham DFT, the xc approximation enters the self-consistent field (SCF) equations through a first derivative (the potential contribution), while in adiabatic LR-TDDFT, it further enters through a second derivative (the response kernel) that governs excitation energies in the Casida formulation.

A central difficulty is that the same xc approximation must simultaneously control energies, SCF potentials, and LR kernels. Most traditional functionals are parameterized primarily against ground-state data, and their transferability to excited states is therefore not guaranteed. [5–9] A common workaround is to tune parameters (e.g., range-separation or hybrid mixing) for a specific system or class of systems to improve selected excitation energies, at the cost of reduced transferability. [10, 11] This limitation becomes even more acute for data-driven functionals [12–16], though previous works were done on the ground state: for example, DeepKS achieves substantially improved force accuracy only when forces are included explicitly as training targets, rather than emerging automatically from fitting energies alone. [15] Motivated by this observation, we include LR excitation information explicitly in the training objective and optimize the functional end-to-end through both the SCF fixed point and the LR-TDDFT eigenvalue problem.

Recent efforts have begun to apply machine learning to time-dependent density functional theory; for example, by learning time-dependent exchange–correlation potentials from real-time densities in model systems. However, they focus on real-time TDDFT which has much heavier computation costs than LR-TDDFT. [17] In this

work, we focus on a complementary direction: learning an energy functional that is used self-consistently for the ground state and, through automatic differentiation, yields a consistent adiabatic LR kernel for excitation energies. Importantly, we include LR excitation information explicitly in the training objective rather than relying on a functional optimized only for ground-state observables. Additionally, we add some exact constraints for xc functionals in the penalty function. Below, we describe a differentiable SCF + LR-TDDFT training workflow that maintains analytic consistency between the learned energy, potential, and adiabatic kernel, and we demonstrate it in a proof-of-concept setting.

The training of deep learning-based functionals for diverse target properties constitutes a non-trivial problem. A primary difficulty arises from the fact that conventional quantum chemistry packages are inherently non-differentiable. Consequently, it is challenging to derive analytical gradients for each computational step manually. The absence of such gradients precludes the straightforward application of gradient-based optimization methods for direct model training. Several tricks have been proposed to partially solve this problem. One approach is referred to as iterative training.[13, 15] Since the SCF component remains non-differentiable, the overall training protocol cannot be fully optimized via gradient-based methods. Consequently, the loss function may increase between successive iterations, and training on different target quantities often necessitates the use of distinct ad hoc techniques. Another strategy involves performing the training directly on the xc potential [18], which is obtained via the Wu–Yang inversion procedure [19]. In this framework, the model is trained using highly accurate reference electron densities. However, during the self-consistent field (SCF) iterations, the evolving density can deviate substantially from the training density, which may induce numerical instabilities and conver-

gence difficulties in the SCF procedure. To enable robust and stable training, we implement a fully differentiable quantum chemistry package, IQC (intelligent quantum chemistry), which supports two-component DFT [20, 21] and two-component TDDFT [22, 23]. A key to making the program differentiable is implementing the two quantum chemistry methods in the framework of JAX [24]. Three pertinent software packages, JAXDFT [25], DQC [16, 26] and PySCFAD [27], have been introduced in the literature. However, none of them currently implement the two methods considered in this work. JAXDFT and DQC are limited to one-component DFT. PySCFAD is limited to one-component DFT and closed-shell one-component TDDFT. Furthermore, the capabilities of PySCFAD have not been validated in the context of training xc functionals.

A concise overview of the two-component formulations of DFT and LR-TDDFT is provided here. We use Γ, Λ, Θ for two-component AO basis functions, P, Q, R for two-component molecular orbitals, and $I, J, K / A, B, C$ for occupied / virtual orbitals.

The molecular orbitals are expressed in terms of two-component bases,

$$P = C_{\Lambda P} \Lambda \quad (1)$$

where $C_{\Lambda P}$ are the expansion coefficients of the orbital P in the basis Λ .

The first-order reduced density matrix is defined as follows:

$$D_{\Lambda \Gamma} = C_{\Lambda I}^* C_{\Gamma I} \quad (2)$$

The matrix representation of the Fock operator for two-component DFT is given by:

$$F_{\Gamma \Lambda} = h_{\Gamma \Lambda} + (\Gamma \Lambda | \Pi \Theta) D_{\Theta \Pi} - c_{\text{HF}}(\Gamma \Theta | \Pi \Lambda) D_{\Theta \Pi} + \frac{\partial E_{\text{xc}}}{\partial D_{\Gamma \Lambda}} \quad (3)$$

By applying partial differentiation to the Fock matrix with respect to the density matrix, we obtain the matrix representation of the kernel operator:

$$K_{\Gamma \Lambda \Theta \Pi} = (\Gamma \Lambda | \Pi \Theta) - c_{\text{HF}}(\Gamma \Theta | \Pi \Lambda) + \frac{\partial^2 E_{\text{xc}}}{\partial D_{\Gamma \Lambda} \partial D_{\Pi \Theta}} \quad (4)$$

The two-component KS-DFT equation reads as follows:

$$FC = SC\epsilon \quad (5)$$

Here, S is the overlap matrix in a set of two-component basis functions. ϵ is a diagonal matrix representing the orbital energies. By solving this equation within the self-consistent field (SCF) framework, we obtain the ground-state wavefunctions. Furthermore, to perform TDDFT calculations, it is necessary to first carry out a DFT calculation to determine the wavefunctions of the reference state.

The Casida equation for TDDFT reads as follows:

$$\begin{pmatrix} H_{AIBJ} & H_{AIJB} \\ H_{IABJ} & H_{IAJB} \end{pmatrix} \begin{pmatrix} X_{BJ} \\ X_{JB} \end{pmatrix} = \begin{pmatrix} 1 & 0 \\ 0 & -1 \end{pmatrix} \begin{pmatrix} X_{AI} \\ X_{IA} \end{pmatrix} \Omega \quad (6)$$

where

$$\begin{pmatrix} H_{AIBJ} & H_{AIJB} \\ H_{IABJ} & H_{IAJB} \end{pmatrix} = \begin{pmatrix} F_{AB} \delta_{IJ} - F_{JI} \delta_{AB} & 0 \\ 0 & F_{BA} \delta_{IJ} - F_{IJ} \delta_{AB} \end{pmatrix} + \begin{pmatrix} K_{AIBJ} & K_{AIJB} \\ K_{IABJ} & K_{IAJB} \end{pmatrix} \quad (7)$$

In this work, we set H_{AIJB} and H_{IABJ} to be zero, which is referred to as the Tamm-Dancoff approximation (TDA). [28] Here, the fock and kernel are both under MO representation, which can be easily transformed from AO representation. In this work, we focus on adiabatic LR-TDDFT, where the response kernel is obtained as the second derivative of the same energy functional used in the ground-state calculation. The frequency dependence (memory effects) of the exact TDDFT kernel is beyond the present scope; [29] our goal here is to enable joint optimization of ground-state and LR excitation targets while maintaining analytic consistency between the learned energy, potential, and adiabatic kernel.

There are two technical problems with backward differentiation. A problem is calculating backward gradients in SCF. Prior approaches have employed a fixed number of linear mixing iterations to enforce self-consistency, relying on the automatic differentiation framework to back-propagate gradients through the entire sequence of iterations. [25, 30] However, a straightforward unrolling of the procedure may generate ill-defined intermediate states and lead to excessive memory consumption, which limits the two works to very small systems such as H_2 . We instead treat the converged SCF solution as the root of a fixed-point equation in Fock space. Let \mathcal{S}_θ denote one SCF update that maps an input Hermitian Fock matrix F to an output Fock matrix F^{out} by (i) solving the generalized eigenproblem in Eq. (5) to obtain the density matrix $D(F)$ and (ii) rebuilding the Fock matrix from $D(F)$, including the learned functional parameters θ . Note that \mathcal{S}_θ doesn't include the step of mixing in SCF. The self-consistent solution $F^*(\theta)$ satisfies

$$g(F, \theta) \equiv \mathcal{S}_\theta(F) - F = 0. \quad (8)$$

Gradients of any scalar objective that depends on the SCF solution are obtained by implicit differentiation of Eq. (8), which reduces the backward pass to solving an adjoint linear system involving the Jacobian of g ; this avoids unrolling and keeps the memory cost independent of the number of SCF iterations. Full derivations and numerical details are provided in the Supplemental Material. Another issue arises in the evaluation of gradients of the eigendecomposition in the presence of (near-)degenerate eigenvalues, which is prevalent in solving the

KS equation and the Casida equation. The main difficulty is to circumvent terms of the form $\frac{1}{\Delta_{PQ}}$, where Δ_{PQ} denotes the gap between two eigenvalues P and Q . [31] To regularize this expression when Δ_{PQ} is very small, we replace it with $\frac{\Delta_{PQ}}{\Delta_{PQ}^2 + \epsilon}$, where ϵ is a small perturbative parameter that is set to 10^{-12} in this work.

On the basis of the aforementioned equations, the evaluation of $\frac{\partial E_{xc}}{\partial D_{\Gamma\Lambda}}$ and $\frac{\partial^2 E_{xc}}{\partial D_{\Gamma\Lambda} \partial D_{\Pi\Theta}}$ constitutes the central step of this workflow. In the present implementation, we adopt full exact exchange ($c_{HF} = 1$). Accordingly, the neural network term in Eqs. (3)-(4) represents an effective exchange-correlation energy functional (a learned exchange-correction beyond Hartree–Fock exchange), although we keep the symbol for notational consistency with the standard DFT expressions, from which the Fock matrix and response kernel are obtained via partial differentiation. A schematic representation of the DFT and TDDFT workflows incorporating a deep-learning-based exchange–correlation functional, namely IXC, is provided in Figure 1. In the figure, D , F , and K refer to the density matrix, Fock matrix, and kernel, respectively. E_{xc} appears in three distinct stages of the calculation: in the evaluation of the total electronic energy; in the construction of the Fock matrix during the self-consistent field (SCF) procedure; and in the construction of both the Fock matrix and the response kernel matrix after SCF convergence has been achieved. Subsequently, by solving the Casida equation, one can obtain the excitation energies and related properties of the electronically excited states. In a fixed finite atomic-orbital basis, the one-particle density matrix D provides a compact representation of the electron density within that basis. In this proof-of-concept study, we use the eigenvalue spectrum of D as a rotationally invariant and variable-length descriptor for the neural network. We emphasize that the spectrum is a compressed representation and does not uniquely specify the full matrix D ; therefore, the present model should be viewed as a minimal, basis-set-specific construction aimed at demonstrating differentiable self-consistent training across DFT and LR-TDDFT. To handle variable-length inputs, we apply a shared per-eigenvalue embedding multilayer perceptron (MLP) and aggregate features by mean pooling, followed by a small prediction head that outputs a scalar energy correction. This simple pooling choice does not formally enforce strict size-extensivity, which we discuss as a limitation and an important direction for future work. Both multilayer perceptrons (MLPs) have two hidden layers, each with 32 units. Calculations were performed using the cc-pVDZ basis set throughout this work.

By employing the eigenvalues as input features, rotational invariance with respect to rigid molecular rotations is inherently ensured. More advanced requirements involve satisfying exact constraints on xc functionals. Because it is highly nontrivial to construct a neural network

that rigorously satisfies these constraints for arbitrary parameter values, we instead incorporate the constraints into the loss (penalty) function, a strategy that is, in principle, applicable to an arbitrary set of constraints. In this work, we focus on two such constraints. The first constraint is one-electron self-interaction cancelation. For any one-electron density, the exact condition implies that the electron–electron interaction is fully canceled by exchange–correlation, and correlation vanishes. Under our choice of full exact exchange ($c_{HF} = 1$), this reduces to requiring that the learned exchange–correlation contribution does not spuriously lower the energy of one-electron systems. We enforce this by penalizing the deviation of the IXC total energy from the Hartree–Fock energy for He^+ . The other one is the Lieb–Oxford bound [32], which reads as:

$$\Delta_{\text{LO}} = \tilde{E}_{\text{xc}} + 1.68 \int \rho^{\frac{4}{3}}(\mathbf{r}) d\mathbf{r} > 0 \quad (9)$$

Note that \tilde{E}_{xc} encompasses the complete exchange and correlation contributions, and therefore differs from the previously defined E_{xc} . More specifically, in this work, $\tilde{E}_{\text{xc}} = E_{\text{x}}^{\text{HF}} + E_{\text{xc}}^{\text{NN}}$. We adopt the original Lieb–Oxford constant 1.68 for a conservative universal bound; tighter estimates (e.g., 1.6358) have been reported in the literature [33] and can be incorporated straightforwardly into the same penalty framework.

The training for this work is conducted on a single atom He, whose loss function is defined as:

$$L = c_1 \frac{1}{n} \sum_k (\Omega_k(\text{He}) - \Omega_k^{\text{T}}(\text{He}))^2 + c_2 [\text{SIE}(\text{He}^+)]^2 + c_3 [\ln(1 + e^{-\Delta_{\text{LO}}(\text{He})})]^2 \quad (10)$$

Here, Ω_k is the k -th excitation energy calculated by our DFT and TDDFT procedures using our deep learning functional IXC. Ω_k^{T} is the targeted k -th excitation energy. SIE (self-interaction error) is defined as the deviation of the total energy of a one-electron system from the corresponding Hartree–Fock reference value. For the helium cation, this quantity is given by

$$\text{SIE}(\text{He}^+) = |E(\text{He}^+) - E_{\text{HF}}(\text{He}^+)| \quad (11)$$

where $E(\text{He}^+)$ denotes the computed total energy of He^+ and $E_{\text{HF}}(\text{He}^+)$ is the Hartree–Fock total energy of the same system. Hyperparameters are chosen as: $c_1 = 10$, $c_2 = 1$, and $c_3 = 10^{-4}$. The Adam optimizer is used, and the learning rate is fixed at 10^{-4} . Weights are initialized with LeCun-normal kernels and zero biases (fixed RNG seed). We consider the two lowest excited states S_1 and T_1 . Degeneracy among states with the same spin multiplicity is a vital point here. If the xc energy functional is invariant under global spin rotation, this degeneracy will be preserved. [34] Because we use the eigenvalues of the density matrix as input, this degeneracy is strictly

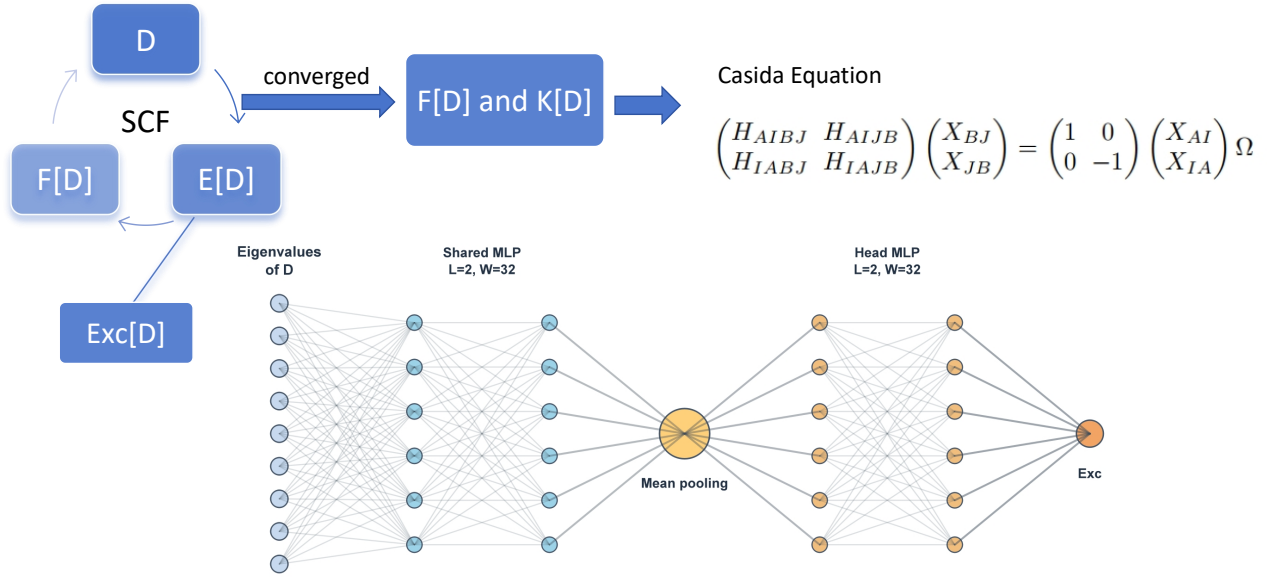


FIG. 1. End-to-end DFT and LR-TDDFT differentiable workflow. A learned xc energy functional is used self-consistently in SCF; its first and second derivatives provide a consistent potential contribution and an adiabatic LR kernel via automatic differentiation. Gradients are propagated through the SCF fixed point by implicit differentiation and through the TDDFT eigenproblem by differentiating the LR eigenvalue solution.

preserved. Note that Ω_n refers to a distinct excitation energy. For example, T_1 is counted once in the loss function rather than three times. Targeted excitation energies are acquired using two-component EOM-CCSD. [35, 36]

In Fig. 2, we report the evolution of the total loss during training, together with the deviations of $\Omega(S_1)$, $\Omega(T_1)$, and SIE from the reference values obtained with the highly accurate EOM-CCSD method. For comparison, we also show the corresponding results obtained with HF, SVWN, PBE, and B3LYP in LR-TDDFT. It should be noted that all traditional functionals employed in this work are noncollinear generalizations of the corresponding collinear functionals, constructed via the multi-collinear approach. [20, 21] The entire training procedure converges within only ten iterations, and the total training loss decreases in a smooth and monotonic manner, indicating substantially enhanced efficiency and predictive performance relative to alternative training strategies. For the first singlet excited state S_1 , the SVWN, PBE, B3LYP, and IXC functionals all exhibit deviations smaller than 0.01 au. For the first triplet excited state T_1 , both B3LYP and IXC yield deviations below 0.01 au. For the self-interaction error in the He^+ system, B3LYP and IXC produce very small deviations, below 0.005 au. Δ_{LO} remains positive during training. The accuracy achieved

by the trained IXC functional demonstrates that the proposed training protocol is capable of accurately fitting a diverse set of properties.

In Table I, we report the performance of our trained IXC functional, which employs HF as its baseline, for three mindlessly chosen systems H_2 , Li^+ , and H_2O . Their geometries are shown in the Supplementary Materials. The results are compared with those obtained using the reference HF, SVWN, PBE, and B3LYP functionals. Four properties are evaluated: $\Omega(S_1)$, $\Omega(T_1)$, the self-interaction error (SIE), and Δ_{LO} . The SIE is computed for the corresponding one-electron ion associated with each system; for example, the SIE for H_2 is evaluated using H_2^+ . For the mean absolute error (MAE), the IXC, HF, and B3LYP functionals all exhibit deviations smaller than 0.1 au, while IXC, in particular, shows a much smaller deviation in the SIE, below 0.01 au. For the MAE, the IXC shows superior accuracy compared to the commonly used hybrid functional B3LYP. This benchmark demonstrates the potential transferability of our training strategy, even though IXC is trained on a single atom and with a fixed basis set.

In summary, we presented a fully differentiable workflow that enables gradient-based training of a single energy functional using both self-consistent ground-state

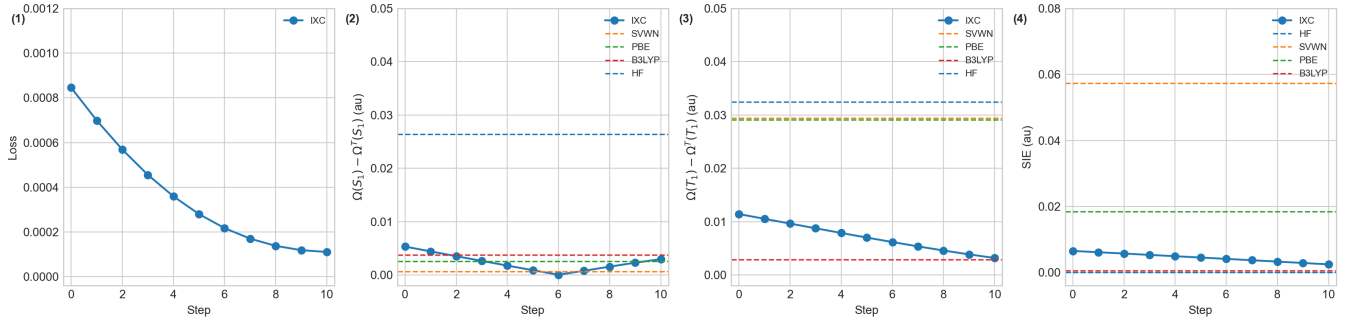


FIG. 2. The evolution of four quantities during the training on He: (1) the total training loss; (2) the deviation of the S_1 excitation energy; (3) the deviation of the T_1 excitation energy; and (4) the self-interaction error for He^+ . Compared data acquired by HF, SVWN, PBE, and B3LYP is presented as dashed lines.

Entry	Functional	$\Omega(S_1)$	$\Omega(T_1)$	SIE	Δ_{LO}
H_2	HF	0.517271	0.371034	0	0.629
	SVWN	0.490167	0.388046	0.029251	0.619
	PBE	0.497702	0.379487	0.006926	0.599
	B3LYP	0.502249	0.383736	0.000863	0.586
	IXC	0.558967	0.396410	0.003025	0.626
	Target	0.511648	0.392869	0	>0
Li^+	HF	2.273030	2.236530	0	1.579
	SVWN	1.953619	1.925308	0.084616	1.667
	PBE	1.990289	1.954699	0.029828	1.554
	B3LYP	2.056259	2.020726	0.002445	1.526
	IXC	2.273623	2.237941	0.001410	1.583
	Target	2.261879	2.236319	0	>0
H_2O	HF	0.338660	0.304693	0	9.523
	SVWN	0.273422	0.250204	0.295959	9.693
	PBE	0.270693	0.245600	0.0433	9.223
	B3LYP	0.280665	0.254333	0.028856	9.144
	IXC	0.342822	0.308343	0.003333	9.533
	Target	0.300572	0.275716	0	>0
MAE	HF	0.018287	0.017008	0.000000	
	SVWN	0.118964	0.113782	0.136609	
	PBE	0.105138	0.108373	0.026685	
	B3LYP	0.078309	0.082036	0.010721	
	IXC	0.033771	0.012597	0.002589	

TABLE I. Performance on H_2 , Li^+ and H_2O of our trained IXC functional (employing HF as its baseline functional), in comparison with HF, SVWN, PBE, and B3LYP functionals. Referenced excitation energies are acquired by two-component EOM-CCSD. All units are au. Basis set is chosen as cc-pVDZ.

and adiabatic LR excitation targets. By implementing two-component DFT and LR-TDDFT in a JAX-based code and deriving the potential and response kernel by automatic differentiation, the approach enforces analytic consistency across energy, SCF, and linear response. The present implementation uses a minimal spectral descriptor of the density matrix in a fixed finite basis and incorporates one-electron self-interaction cancelation and the Lieb–Oxford inequality via penalty terms. Extending the descriptor set, enforcing strict size-extensivity by

construction, using more diverse training sets, and moving beyond the adiabatic approximation are promising directions for future work.

Xiaoyu Zhang gratefully acknowledges the encouragement provided by Yunlong Xiao. In addition, Xiaoyu Zhang thanks Yixiao Chen for his early-stage yet valuable discussions.

* zhangxiaoyu@stu.pku.edu.cn

- [1] P. Hohenberg and W. Kohn, “Inhomogeneous electron gas,” *Phys. Rev.* **136**, B864–B871 (1964).
- [2] W. Kohn and L. J. Sham, “Self-consistent equations including exchange and correlation effects,” *Phys. Rev.* **140**, A1133–A1138 (1965).
- [3] Erich Runge and E. K. U. Gross, “Density-functional theory for time-dependent systems,” *Phys. Rev. Lett.* **52**, 997–1000 (1984).
- [4] Mark E. Casida, “Time-dependent density functional response theory for molecules,” (1995) pp. 155–192.
- [5] John P. Perdew and Karla Schmidt, “Jacob’s ladder of density functional approximations for the exchange-correlation energy,” *AIP Conference Proceedings* **577**, 1–20 (2001).
- [6] John P. Perdew, Adrienn Ruzsinszky, Jianmin Tao, Viktor N. Staroverov, Gustavo E. Scuseria, and Gábor I. Csonka, “Prescription for the design and selection of density functional approximations: More constraint satisfaction with fewer fits,” *The Journal of Chemical Physics* **123**, 062201 (2005).
- [7] Narbe Mardirossian and Martin Head-Gordon, “Thirty years of density functional theory in computational chemistry: an overview and extensive assessment of 200 density functionals,” *Molecular Physics* **115**, 2315–2372 (2017).
- [8] Yan Zhao and Donald G. Truhlar, “The m06 suite of density functionals for main group thermochemistry, thermochemical kinetics, noncovalent interactions, excited states, and transition elements: two new functionals and systematic testing of four m06-class functionals and 12 other functionals,” *Theoretical Chemistry Accounts* **120**, 215–241 (2008).

[9] Takeshi Yanai, David P Tew, and Nicholas C Handy, “A new hybrid exchange–correlation functional using the coulomb-attenuating method (cam-b3lyp),” *Chemical Physics Letters* **393**, 51–57 (2004).

[10] Katsuki Okuno, Yasuteru Shigeta, Ryohei Kishi, Hiroshi Miyasaka, and Masayoshi Nakano, “Tuned cam-b3lyp functional in the time-dependent density functional theory scheme for excitation energies and properties of diarylethene derivatives,” *Journal of Photochemistry and Photobiology A: Chemistry* **235**, 29–34 (2012).

[11] Leeor Kronik, Tamar Stein, Sivan Refaelly-Abramson, and Roi Baer, “Excitation gaps of finite-sized systems from optimally tuned range-separated hybrid functionals,” *Journal of Chemical Theory and Computation* **8**, 1515–1531 (2012), pMID: 26593646, <https://doi.org/10.1021/ct2009363>.

[12] Jiang Wu, Sai-Mang Pun, Xiao Zheng, and Guan-Hua Chen, “Construct exchange-correlation functional via machine learning,” *The Journal of Chemical Physics* **159**, 090901 (2023).

[13] Sebastian Dick and Mariy Fernandez-Serra, “Machine learning accurate exchange and correlation functionals of the electronic density,” *Nature Communications* **11**, 3509 (2020).

[14] James Kirkpatrick, “Pushing the frontiers of density functionals by solving the fractional electron problem,” *Science* **374** (2021), 10.1126/science.abj6511.

[15] Yixiao Chen, Linfeng Zhang, Han Wang, and Weinan E, “Deepks: A comprehensive data-driven approach toward chemically accurate density functional theory,” *Journal of Chemical Theory and Computation* **17**, 170–181 (2021), pMID: 33296197, <https://doi.org/10.1021/acs.jctc.0c00872>.

[16] M. F. Kasim and S. M. Vinko, “Learning the exchange-correlation functional from nature with fully differentiable density functional theory,” *Phys. Rev. Lett.* **127**, 126403 (2021).

[17] Yasumitsu Suzuki, Ryo Nagai, and Jun Haruyama, “Machine learning exchange-correlation potential in time-dependent density-functional theory,” *Phys. Rev. A* **101**, 050501 (2020).

[18] Yi Zhou, Jiang Wu, Shuguang Chen, and GuanHua Chen, “Toward the exact exchange–correlation potential: A three-dimensional convolutional neural network construct,” *The Journal of Physical Chemistry Letters* **10**, 7264–7269 (2019), pMID: 31690079.

[19] Qin Wu and Weitao Yang, “A direct optimization method for calculating density functionals and exchange–correlation potentials from electron densities,” *The Journal of Chemical Physics* **118**, 2498–2509 (2003).

[20] Zhichen Pu, Hao Li, Ning Zhang, Hong Jiang, Yiqin Gao, Yunlong Xiao, Qiming Sun, Yong Zhang, and Sihong Shao, “Noncollinear density functional theory,” *Phys. Rev. Res.* **5**, 013036 (2023).

[21] Xiaoyu Zhang and Taoni Bao, “Operator formalism for noncollinear functionals in the multicollinear approach,” *Journal of Chemical Theory and Computation* **21**, 9620–9630 (2025), pMID: 41039659, <https://doi.org/10.1021/acs.jctc.5c01305>.

[22] Hao Li, Zhichen Pu, Qiming Sun, Yi Qin Gao, and Yunlong Xiao, “Noncollinear and spin-flip tddft in multicollinear approach,” *Journal of Chemical Theory and Computation* **19**, 2270–2281 (2023).

[23] Xiaoyu Zhang, Tai Wang, Yi Qin Gao, and Yunlong Xiao, “Noncollinear spin-flip tddft for potential energy surface crossings: Conical intersections and spin crossings,” *Journal of Chemical Theory and Computation* **21**, 11550–11561 (2025), pMID: 41208132, <https://doi.org/10.1021/acs.jctc.5c01272>.

[24] Roy Frostig, Matthew Johnson, and Chris Leary, “Compiling machine learning programs via high-level tracing,” (2018).

[25] Li Li, Stephan Hoyer, Ryan Pederson, Ruoxi Sun, Ekin D. Cubuk, Patrick Riley, and Kieron Burke, “Kohn–sham equations as regularizer: Building prior knowledge into machine-learned physics,” *Phys. Rev. Lett.* **126**, 036401 (2021).

[26] Muhammad F. Kasim, Susi Lehtola, and Sam M. Vinko, “Dqc: A python program package for differentiable quantum chemistry,” *The Journal of Chemical Physics* **156**, 084801 (2022).

[27] Xing Zhang and Garnet Kin-Lic Chan, “Differentiable quantum chemistry with pyscf for molecules and materials at the mean-field level and beyond,” *The Journal of Chemical Physics* **157**, 204801 (2022).

[28] So Hirata and Martin Head-Gordon, “Time-dependent density functional theory within the tamm–dancoff approximation,” *Chemical Physics Letters* **314**, 291–299 (1999).

[29] Giovanni Onida, Lucia Reining, and Angel Rubio, “Electronic excitations: density-functional versus many-body green’s-function approaches,” *Rev. Mod. Phys.* **74**, 601–659 (2002).

[30] Teresa Tamayo-Mendoza, Christoph Kreisbeck, Roland Lindh, and Alán Aspuru-Guzik, “Automatic differentiation in quantum chemistry with applications to fully variational hartree–fock,” *ACS Central Science* **4**, 559–566 (2018), pMID: 29806002, <https://doi.org/10.1021/acscentsci.7b00586>.

[31] J. A. Pople, R. Krishnan, H. B. Schlegel, and J. S. Binkley, “Derivative studies in hartree–fock and møller–plesset theories,” *International Journal of Quantum Chemistry* **16**, 225–241 (1979), <https://onlinelibrary.wiley.com/doi/pdf/10.1002/qua.560160825>.

[32] Elliott H. Lieb and Stephen Oxford, “Improved lower bound on the indirect coulomb energy,” *International Journal of Quantum Chemistry* **19**, 427–439 (1981), <https://onlinelibrary.wiley.com/doi/pdf/10.1002/qua.560190306>.

[33] Garnet Kin-Lic Chan and Nicholas C. Handy, “Optimized lieb-oxford bound for the exchange–correlation energy,” *Phys. Rev. A* **59**, 3075–3077 (1999).

[34] Tai Wang, Hao Li, Yi Qin Gao, and Yunlong Xiao, “Zero excitation energy theorem and the spin-flip kernel,” *Journal of Chemical Theory and Computation* **21**, 6905–6921 (2025), pMID: 40638888, <https://doi.org/10.1021/acs.jctc.5c00714>.

[35] John F. Stanton and Rodney J. Bartlett, “The equation of motion coupled-cluster method. a systematic biorthogonal approach to molecular excitation energies, transition probabilities, and excited state properties,” *The Journal of Chemical Physics* **98**, 7029–7039 (1993).

[36] Sergey V. Levchenko and Anna I. Krylov, “Equation-of-motion spin-flip coupled-cluster model with single and double substitutions: Theory and application to cyclobutadiene,” *The Journal of Chemical Physics* **120**, 175–185 (2004).

**SUPPLEMENTAL MATERIALS:
END-TO-END DIFFERENTIABLE LEARNING
OF A SINGLE FUNCTIONAL FOR DFT AND
LINEAR-RESPONSE TDDFT**

Implicit differentiation through the SCF fixed point

Let \mathcal{L} be any real-valued scalar objective that depends on the SCF fixed point (and possibly explicitly on θ).

$$\mathcal{L}(\theta) = \tilde{\mathcal{L}}(F^*(\theta), \theta). \quad (12)$$

Differentiating the root condition $g(F^*(\theta), \theta) = 0$ yields

$$\frac{\partial g}{\partial F} \bigg|_{F^*} : dF^* + \frac{\partial g}{\partial \theta} \bigg|_{F^*} d\theta = 0, \quad (13)$$

so that

$$dF^* = - \left(\frac{\partial g}{\partial F} \bigg|_{F^*} \right)^{-1} \frac{\partial g}{\partial \theta} \bigg|_{F^*} d\theta. \quad (14)$$

Directly forming the inverse in Eq. (14) is unnecessary. In reverse-mode differentiation, we instead introduce an adjoint (Lagrange multiplier) matrix Λ that solves the transposed/adjoint linear system

$$\left(\frac{\partial g}{\partial F} \bigg|_{F^*} \right)^\dagger \Lambda = \left(\frac{\partial \tilde{\mathcal{L}}}{\partial F} \bigg|_{F^*} \right)^\dagger. \quad (15)$$

Using the Frobenius inner product $\langle A, B \rangle \equiv \text{Re} \text{Tr}(A^\dagger B)$, the total gradient is

$$\frac{d\mathcal{L}}{d\theta} = \frac{\partial \tilde{\mathcal{L}}}{\partial \theta} \bigg|_{F^*} - \left\langle \Lambda, \frac{\partial g}{\partial \theta} \bigg|_{F^*} \right\rangle. \quad (16)$$

Since $g(F, \theta) = \mathcal{S}_\theta(F) - F$, we have

$$\frac{\partial g}{\partial F} = \frac{\partial \mathcal{S}_\theta}{\partial F} - I, \quad \frac{\partial g}{\partial \theta} = \frac{\partial \mathcal{S}_\theta}{\partial \theta}. \quad (17)$$

Equations (15)–(16) are the implicit gradient formulas used to backpropagate through the SCF fixed point.

In practice, we never construct $\partial g / \partial F$ explicitly. For any matrix perturbation V in the space of F , the Jacobian–vector product is evaluated as a directional derivative,

$$\left(\frac{\partial g}{\partial F} \bigg|_{F^*} \right) V = \frac{d}{d\epsilon} g(F^* + \epsilon V, \theta) \bigg|_{\epsilon=0}, \quad (18)$$

which is obtained by automatic differentiation of the single-step map \mathcal{S}_θ . The adjoint system in Eq. (15) is solved iteratively using a stationary fixed-point iteration for the linear equation $AX = B$, accelerated using DIIS (Anderson acceleration).

Geometries of H₂ and H₂O

Unit: Angstrom

H₂:
H 0, 0, 0.74
H 0, 0, 0

H₂O:
O 0, 0, 0
H 0, 0.757, 0.587
H 0, -0.757, 0.587